Biophysical Journal
Article

Biophysical Society

# PIP Water Transport and Its pH Dependence Are Regulated by Tetramer Stoichiometry

Cintia Jozefkowicz,[1] Lorena Sigaut,[2,3] Florencia Scochera,[1,4] Gabriela Soto,[5] Nicolás Ayub,[5] Lía Isabel Pietrasanta,[2,3,6] Gabriela Amodeo,[7] F. Luis González Flecha,[1] and Karina Alleva[1,4,*]

[1]Instituto de Química y Fisicoquímica Biológica Alejandro C. Paladini (IQUIFIB), Universidad de Buenos Aires, Consejo National de Investigaciones Científicas y Técnicas (UBA-CONICET), Buenos Aires, Argentina; [2]Departamento de Física, Facultad de Ciencias Exactas y Naturales, Universidad de Buenos Aires, Buenos Aires, Argentina; [3]Instituto de Física de Buenos Aires (IFIBA), CONICET, Ciudad Universitaria, Buenos Aires, Argentina; [4]Departamento de Fisicomatemática, Facultad de Farmacia y Bioquímica, Universidad de Buenos Aires, Buenos Aires, Argentina; [5]Instituto de Genética Ewald A. Favret, Centro de Investigación en Ciencias Veterinarias y Agronómicas, Instituto Nacional de Tecnología Agropecuaria (INTA), Castelar, Argentina; [6]Centro de Microscopías Avanzadas, Facultad de Ciencias Exactas y Naturales and [7]Departamento de Biodiversidad y Biología Experimental, Instituto de Biodiversidad y Biología Experimental y Aplicada, Facultad de Ciencias Exactas y Naturales, UBA-CONICET, Buenos Aires, Argentina

ABSTRACT Many plasma membrane channels form oligomeric assemblies, and heterooligomerization has been described as a distinctive feature of some protein families. In the particular case of plant plasma membrane aquaporins (PIPs), PIP1 and PIP2 monomers interact to form heterotetramers. However, the biological properties of the different heterotetrameric configurations formed by PIP1 and PIP2 subunits have not been addressed yet. Upon coexpression of tandem PIP2-PIP1 dimers in *Xenopus* oocytes, we can address, for the first time to our knowledge, the functional properties of single heterotetrameric species having 2:2 stoichiometry. We have also coexpressed PIP2-PIP1 dimers with PIP1 and PIP2 monomers to experimentally investigate the localization and biological activity of each tetrameric assembly. Our results show that PIP2-PIP1 heterotetramers can assemble with 3:1, 1:3, or 2:2 stoichiometry, depending on PIP1 and PIP2 relative expression in the cell. All PIP2-PIP1 heterotetrameric species localize at the plasma membrane and present the same water transport capacity. Furthermore, the contribution of any heterotetrameric assembly to the total water transport through the plasma membrane doubles the contribution of PIP2 homotetramers. Our results also indicate that plasma membrane water transport can be modulated by the coexistence of different tetrameric species and by intracellular pH. Moreover, all the tetrameric species present similar cooperativity behavior for proton sensing. These findings throw light on the functional properties of PIP tetramers, showing that they have flexible stoichiometry dependent on the quantity of PIP1 and PIP2 molecules available. This represents, to our knowledge, a novel regulatory mechanism to adjust water transport across the plasma membrane.

## INTRODUCTION

The specific self-association of membrane channels to form oligomeric assemblies is a biologically relevant event that usually confers functional advantages to biological systems. Aquaporins (AQPs) are transmembrane channels organized as tetramers, where each monomer can transport water (1). There are seven AQP subfamilies in the plant kingdom, but only four of those are widely distributed in flowering plants: plasma membrane intrinsic proteins (PIPs), tonoplast intrinsic proteins, nodulin 26-like intrinsic membrane proteins, and small and basic intrinsic proteins (2). PIPs are the only plant aquaporins whose structure has been resolved. Kukulski et al. (3) resolved, by crystal electron diffraction, the structure of SoPIP2;1 and demonstrated, by superposition of the SoPIP2;1 potential map with the atomic model of AQP1, that the overall structure of both channels was generally well conserved.

PIPs are divided into two groups, PIP1 and PIP2, which have significant sequence identity with major differences in the N- and C- tails and loop A (the first extracellular loop), and SoPIP2;1 and SoPIP1;2 were first revealed in a tetrameric conformation by scanning transmission electron microscopy mass analysis (4). In particular, members of the PIP subfamily have been intensively studied in recent years as key regulators of plasma membrane water transport due to their capacity to heterooligomerize (5–7). Despite the structural and amino acid similarity found in all PIPs, PIP1 and PIP2 show important functional differences. Although

*Submitted August 3, 2015, and accepted for publication January 19, 2016.*

*Correspondence: kalleva@ffyb.uba.ar

Editor: Ernest Wright.

http://dx.doi.org/10.1016/j.bpj.2016.01.026

PIP2s are usually located in the plasma membrane, most PIP1s are retained in the endoplasmic reticulum (8). Specific sequence motifs controlling PIP1 and PIP2 differential behavior have been described. In maize (*Zea mays*), the motif LxxxA, located in transmembrane domain 3 (TM3), and an N-terminal endoplasmic-reticulum-export diacidic motif can account for the differential localization of some of these proteins (9–11).

Regardless of the different localization of PIP1 and PIP2 when they are expressed alone, PIP1 localization can be modified, and PIP1s can reach the plasma membrane when coexpressed with some PIP2s as a consequence of their physical interaction (5,6,12,13). Indeed, in plants, both PIP1 and PIP2 are found in the same membrane (14–16). However, this kind of interaction seems not to be a general rule for any PIP1 and PIP2. For example, BvPIP2;1 from red beet (*Beta vulgaris*) is unable to promote the incorporation of BvPIP1;1 in the plasma membrane, in contrast to BvPIP2;2 (13). In the case of tobacco PIPs, the interaction of NtAQP1 and NtPIP2;1 does not increase plasma membrane water transport but has proven to impact on their transport selectivity between water and $CO_2$ transport; interestingly enough, maximum rates of $CO_2$ transport were found when artificial tetramers consisted of NtAQP1 only (5). The coexpression of PIP1 and PIP2 also has been shown to modify proton sensing—producing closure of the pore from the cytosolic side at different intracellular pH (17)—and PIP2 monomers modify intrinsic water permeability (6). Some reports have pointed out the relevance of PIP interaction in planta; for example, confocal imaging has shown that the endoplasmic reticulum-retained AtPIP2;1-green-fluorescent-protein (GFP) construct (carrying the mutation E6D) retains AtPIP1;4-mCherry intracellularly, suggesting an interaction between PIP1 and PIP2 in the plant cell (10). These findings highlight the relevance of PIP1-PIP2 interaction for plant cell physiology.

When PIP heterotetramerization is analyzed in the context of channel oligomerization, similar mechanisms of regulation are found. There are, for example, striking similarities between the oligomerization of plant PIP and plant $K^+$ channels. AtKC1 has been reported to be retained in the endoplasmatic reticulum when expressed alone (18–20), although upon coexpression, AKT1 and AtKC1 form active heterotetramers at the plasma membrane (21), modulating $K^+$ influx in root hairs (22). The interaction between AKT1 and AtKC1 channels is similar to that described for PIP1 and PIP2. However, PIP heterotetramerization is still far from understood, since neither the localization nor the biological activity or regulation of PIP heterotetramers with different stoichiometries have been described so far. Until now, only tobacco PIP heterotetramers have been artificially constructed to be studied individually, but those aquaporins do not interact to increase plasma membrane water transport (7).

In this work, we aimed to elucidate the stoichiometric organization of heterotetramers formed by BvPIP2;2 and BvPIP1;1, characterizing their biological activity in terms of water transport. First, we investigated the biological properties of a single heterotetrameric species with 2:2 stoichiometry by expressing tandem PIP2-PIP1 heterodimers. Then, we expressed heterodimers plus PIP2 or PIP1 monomers to analyze the localization of other stoichiometric species different from the 2:2 species. Finally, we characterized their water transport permeability and cooperativity under cytosolic acidification.

## MATERIALS AND METHODS

### DNA constructions

Plasma-membrane intrinsic proteins BvPIP2;2 (GenBank: GQ227846.1) and BvPIP1;1 (GenBank: GQ227845.1) from *Beta vulgaris*—cloned into BglII and SpeI sites of a pT7Ts-derived vector containing T7 RNA polymerase promoter and carrying the 5′ and 3′ translated regions of the *Xenopus laevis* $\beta$ globin gene were used in this study. Enhanced yellow fluorescent protein (EYFP) and enhanced cyan fluorescent protein (ECFP) were genetically attached to the carboxyterminal end of BvPIP2;2 and BvPIP1;1, respectively, as previously described (13). The fluorescently tagged BvPIP2;2 and BvPIP1;1 subunits had linkers of 19 amino acids and 13 amino acids, respectively, between the channel and the fluorescent protein. The EYFP- and ECFP-tagged channels exhibited functional behaviors indistinguishable from those without fluorescence protein tags (13).

Artificial heterodimers containing BvPIP2;2 covalently linked to BvPIP1;1 (referred to as heterodimers in the Results and Discussion) or BvPIP1;1 covalently linked to BvPIP2;2 were synthesized by PCR amplification of *SacII*-BvPIP1;1-*SpeI* or *SacII*-BvPIP2;2-*SpeI*, respectively, purification of the amplified fragment, and ligation into the digested pT7Ts-derived vector containing *SacII* and *SpeI* sites downstream from BvPIP2;2 or BvPIP1;1 cDNA (lacking its stop codon). The BvPIP2;2-BvPIP1;1 and BvPIP1;1-BvPIP2;2 heterodimer constructs contain 19 and 11 amino acids, respectively, between the coding regions of the two PIPs, and special attention was paid to maintain the correct reading frame. All constructs were confirmed by DNA sequencing (MacrogenInc, Rockville, MD) before use.

### In vitro RNA synthesis

The capped complementary RNA (cRNA) encoding BvPIP1;1, BvPIP2;2, heterodimer, and monomers fused to EYFP or ECFP was synthesized in vitro using the mMESSAGE mMACHINE T7 High Yield Capped RNA Transcription Kit (Ambion, Austin, Texas) as described previously (13). The synthesized products were suspended at a final concentration of 0.1 $\mu g\ \mu L^{-1}$ in RNase-free water supplemented with recombinant RNasin (ribonuclease inhibitor, Promega, Madison, WI) and stored at −20°C until use. Agarose gel electrophoresis and GelRed (BioAmerica Biotech, Miami, FL) staining were used to check the absence of unincorporated nucleotides in the cRNA after every in vitro cRNA synthesis. At least four independent cRNA syntheses were assayed. The cRNA was quantified by fluorescence using the Quant-iT RNA Assay Kit (Invitrogen/ThermoFisher Scientific, Waltham, MA,). Results from experiments performed with different oocyte batches were not pooled; therefore, all the experiments shown in this work are representative of at least three different experiments. Before injecting, cRNA was diluted in RNase-free water to inject a proper amount per oocyte. In all figures, the masses of cRNA injected are indicated in parentheses as follows: 0.5 corresponds to 1.25 ng of cRNA; 1 corresponds to 2.5 ng; 2 corresponds to 5 ng; and 4 corresponds to 10 ng injected per oocyte. In some instances, two cRNAs were coinjected in oocytes in different mass ratios, and the same numbers were used to indicate the amount of each cRNA. For example, a 1:1 mass ratio corresponds to 2.5 ng of one cRNA plus 2.5 ng of another cRNA, 1:2 mass ratio corresponds

to 2.5 ng of one cRNA plus 5 ng of another cRNA, and 0.5:2 mass ratio corresponds to 1.25 of one cRNA plus 5 ng of another cRNA. *Xenopus* oocytes were microinjected with a single cRNA or a mixture of cRNAs coding for different PIPs and incubated for three days at 18°C before performing the experiments.

## Oocyte water transport assays

The osmotic water permeability ($P_f$) of oocytes injected or noninjected with cRNA was determined by measuring the rate of oocyte swelling, as explained before (17). Briefly, $P_f$ was determined by measuring the rate of oocyte swelling, induced in response to fivefold dilution of the extracellular buffer with distilled water (extracellular buffer initial osmolarity, ~200 mOsmol $kg^{-1}$ $H_2O$). It was previously demonstrated that the osmotic response of an oocyte is not affected by ion dilution; thus, this experimental design is suitable for water transport experiments (23). Changes in cell volume were video-monitored by a VX-6000 color video-camera (Microsoft, Redmond, WA) attached to a zoom stereo-microscope (Olympus SZ40, Olympus, Tokyo, Japan). Cell swelling was video-captured in still images (10 s each for 60 s) using the AMCaP, version 9.20 (http://noeld.com/programs.asp?cat1/4video#AMCap), and then the images were analyzed by treating each oocyte image as a growing sphere whose volume could be inferred from its cross-sectional area (software Image J, version 1.37, http://rsb.info.nih.gov.ij/).

$P_f$ was calculated according to (23) and (24). Noninjected oocytes were used as negative controls, because no significant differences were found between this condition and water-injected oocytes. All osmolarities were determined using a vapor pressure osmometer (5600C, Wescor, Stoneham, MA).

## Confocal fluorescence microscopy

Confocal fluorescence microscopy was used to localize the respective BvPIP isoforms tagged with ECFP or EYFP in *X. laevis* oocytes. Tetramethylrhodamine (TMR) dextran (10,000 mol wt; Invitrogen/Thermo Fisher Scientific) was used as a marker of the interior of the oocyte, since it is a nonconjugated, nonspecific fluorochrome marker that remains in the cytosol and allows distinction from the plasma membrane (25). Briefly, 3 days after cRNA injection and 40 min before imaging, oocytes were microinjected with 50 nL of a 33 $\mu$M aqueous solution of TMR-dextran. Fluorescence images of ECFP or EYFP distribution together with TMR were obtained with a FluoView1000 spectral confocal scanning microscope (Olympus), using a 60× UPlanSapo oil immersion objective lens NA 1.35. To avoid cross talk, images were recorded line by line in a sequential order. In the case of ECFP and TMR, they were excited using the 458 nm and 515 nm lines of a multiline Argon laser, and the emitted fluorescence was detected in the 475–500 nm and 560–660 nm range, respectively. When EYFP and TMR were used, the 488 nm line of the Argon laser and the 543 nm line of the He-Ne laser were used and the emitted fluorescence was detected in the 500–530 nm and 560–660 nm ranges, respectively. Images were obtained using Kalman filtering. Autofluorescence (monitored in control oocytes) was negligible when compared to cells expressing the fluorescent PIP. We analyzed three to four oocytes for each condition from at least five donor frogs. Intensity profiles were calculated by averaging consecutive pixels over 10 $\mu$m along the direction specified in each figure with ImageJ 1.48v Software (National Institutes of Health, Bethesda, MD).

## pH modulation of oocyte water transport

For pH inhibition experiments, the oocyte internal (cytosolic) pH was modified according to an already described protocol (17). Briefly, the internal pH of oocytes was acidified by preincubating them for 15 min in different pH solutions (NaAc solution: 50 mM NaAc and 20 mM MES for the 5.8–6.8 pH interval or HEPES for the 7.0–7.4 pH interval), supplemented with 1 M mannitol until the desired osmolarity was achieved (~200 mOsmol $kg^{-1}$ $H_2O$). All osmolarities were determined using a vapor pressure osmometer (5600C, Wescor). The swelling response was induced by transferring the oocytes to a fivefold dilution of the same solution with distilled water, keeping the pH of the solution constant. The internal pH was then calculated as described previously (17) and the osmotic water permeability was determined as indicated in a previous section. In all treatments, negative controls were performed by subjecting noninjected oocytes to the same procedure. An empirical sigmoidal function (Eq. 1) was fitted to the experimental data by the nonlinear regression procedure implemented on Excel spreadsheets (26).

$$P_f = P_{f\min} + \left(P_{f\max} - P_{f\min}\right)\frac{K_{0.5}^{n_H}}{K_{0.5}^{n_H} + [H^+]^{n_H}}, \quad (1)$$

where $P_{fmax}$ and $P_{fmin}$ are the asymptotic maximal and minimal values, respectively, of the oocyte water permeability ($P_f$), $K_{0.5}^{n_H}$ is the $[H^+]$ at which the water permeability change is half maximal, and $n_H$ is an empirical coefficient giving account of the mismatch respect to the hyperbolic behavior. Parameter $pH_{0.5}$ is defined as $pH_{0.5} \equiv -\log(K_{0.5})$. The Hill coefficient, $n$, was determined as the maximal value of the first derivative of the Wyman-Hill plot, as described previously (27).

## Data analysis and mathematical modeling

A quantitative model was built to explain the contribution of each tetrameric form to the plasma membrane water permeability, assuming that 1) PIP1 and PIP2 monomers associate as dimers in a first step and the tetramerization occurs by dimerization of dimers, as previously shown for other AQPs (28,29); and 2) the dimerization step is given randomly, allowing different stoichiometries to be assembled. Our experimental data show that 1) PIP biological activity is proportional to the cRNA injected (Fig. S2 in the Supporting Material); and 2) PIP2 homotetramers or PIP1-PIP2 heterotetramers are localized in the plasma membrane, whereas PIP1 homotetramers are not. In the model, we have considered the following types of dimers: X, PIP2-PIP1; Y, PIP1-PIP1; and Z, PIP2-PIP2. Two experimental conditions must be taken into account for the analyses (Fig. S1):

Condition A: injection of PIP1 or PIP2-PIP1 cRNA alone, or PIP1 plus PIP2-PIP1 heterodimers
Condition B: injection of PIP2 or PIP2-PIP1 cRNA alone, or PIP2 plus PIP2-PIP1 heterodimers.

Thus, the possible combinations of dimers to assemble for each kind of coexpression experiments are:

Condition A: X + X (2:2 stoichiometry), Y + Y (0:4 stoichiometry), or X + Y (2:2, 1:3, or 0:4 possible stoichiometries)
Condition B: X + X (2:2 stoichiometry), Z + Z (4:0 stoichiometry), or X + Z (2:2, 3:1, or 4:0 possible stoichiometries).

The proportion of each population of tetramers ($\Phi_i$) containing $i$ subunits can be predicted, in both conditions, by a binomial distribution (28,30–32):

$$\Phi_i = \frac{n!}{i!(n-i)!}\theta^i(1-\theta)^{n-i}, \quad (2)$$

where $n = 2$, $i$ is equal to the number of Y/Z dimers within the tetramer, and $\theta$ is the PIP1/PIP2 molar fraction. Total plasma membrane permeability due to PIP expression ($P_f c$) can be expressed as:

Condition A:

$$P_f c_A = \Omega_{2:2} * \Phi_{i2:2} + \Omega_{1:3} * \Phi_{i1:3} + \Omega_{0:4} * \Phi_{i0:4} \quad (3)$$

Condition B:

$$P_f c_B = \Omega_{2:2} * \Phi_{i2:2} + \Omega_{3:1} * \Phi_{i3:1} + \Omega_{4:0} * \Phi_{i4:0}, \quad (4)$$

where $\Phi_i$ corresponds to the proportion of each population of tetramers containing $i$ Y/Z-dimers obtained from the binomial distribution (Eq. 2), $P_f\ c_{A/B}$ is calculated as (Total $P_f$ measured − $P_f$ of noninjected oocytes)/total ng of injected cRNA, $\Omega$ corresponds to $P_f$ given by the expression of each tetrameric species at the plasma membrane, being $\Omega_{2:2}$, $\Omega_{0:4}$, and $\Omega_{4:0}$ obtained experimentally, whereas $\Omega_{1:3}$ and $\Omega_{3:1}$ are parameters obtained by fitting Eqs. 3 and 4, respectively, to the experimental data by nonlinear regression using GraphPad Prism 5.02 software.

### Statistics

Significant differences between groups were calculated using a two-tailed Student *t*-test or one- way analysis of variance, followed by Tukey's multiple comparison.

## RESULTS AND DISCUSSION

### PIP2-PIP1 heterotetramers with 2:2 stoichiometry show higher water permeability than PIP2 homotetramers but the same cooperative profile for proton sensing

Despite the fact that random heterotetramerization had been previously reported for PIP2 and PIP1, singular heterotetramers of interacting PIP1 and PIP2 that promote water transport increase have not been characterized so far. In this work, we constructed heterodimers encoding for covalently linked BvPIP2;2 and BvPIP1;1 to allow the expression of heterotetramers with two BvPIP2;2 molecules plus two BvPIP1;1 molecules (2:2 stoichiometry) (Fig. S1).

First, we tested the functionality of heterodimers (BvPIP2;2-BvPIP1;1 and BvPIP1;1-BvPIP2;2) and performed water transport assays in *Xenopus* oocytes (Fig. S2). We found that both heterodimers increase the plasma membrane osmotic water permeability coefficient ($P_f$) in a similar way, independent of which monomer was linked by the C-terminal end to the other monomer in the fusion polypeptide. We also found that the $P_f$ values for oocytes injected with either heterodimeric cRNAs (BvPIP2;2-BvPIP1;1 or BvPIP1;1-BvPIP2;2) or BvPIP2;2 are proportional to the cRNA mass injected. These results suggest that the translation machinery of the oocytes was not saturated by these amounts of heterologous cRNAs and responded almost linearly (Fig. S2). In addition, results show that the injection of heterodimer cRNA leads to an increased $P_f$, since a heterotetramer with two BvPIP2;2 molecules plus two BvPIP1;1 molecules (2:2 stoichiometry) is the only tetramer that can be formed. These results allow us to conclude that PIP heterotetramers can be produced by dimerization of heterodimers and that heterotetramers with two BvPIP2;2 molecules plus two BvPIP1;1 molecules (2:2 stoichiometry) are functional.

Interestingly enough, when 5 ng of cRNA coding for the heterodimer is injected in the oocytes, the $P_f$ is not significantly different from what is observed when 2.5 ng of BvPIP2;2 cRNA plus 2.5 ng of BvPIP1;1 cRNA (1:1 cRNA mass ratio) are coinjected; but in those coexpression experiments, several heterotetramer configurations can be formed ($p > 0.05$) (Fig. 1 *A*).

As is well known, the biological activity of PIPs can be inhibited by acidification (33). We observed that the $P_f$ measurements at different intracellular pH values for oocytes expressing the heterodimer presented a behavior well described by a sigmoidal function of proton concentration, a key feature of cooperative processes (Fig. 1 *B*). Three parameters of the fitted curves are relevant to evaluate the molecular events involved in this response: maximal $P_f$, $pH_{0.5}$ (pH at which the half-maximal $P_f$ is found), and the $n$ coefficient (a measure of the degree of cooperativity for proton binding).

When either the heterodimer or BvPIP2;2 cRNA is injected alone into oocytes, single tetrameric species are expressed; in the first case, only heterotetramers with 2:2 stoichiometry are assembled; and in the other case, only BvPIP2;2 homotetramers are formed. When 5 ng of heterodimer cRNA is injected into oocytes, 2:2 heterotetramers are formed and the maximal $P_f$ is $(217.09 \pm 21.16) \times 10^{-4}$ cm $s^{-1}$ (mean ± SE, $n = 5$), the $pH_{0.5}$ is 6.785 ± 0.009 (mean ± SE, $n = 5$), and the $n$ coefficient is 6 (Fig. 1 *B*). In this regard, this is the first report of the $P_f$ response upon internal acidic pH for a plant AQP heterotetramer with 2:2 stoichiometry. When 5 ng of BvPIP2;2 cRNA is injected, only BvPIP2 homotetramers are formed and the maximal $P_f$ is $(89.40 \pm 14.52) \times 10^{-4}$ cm $s^{-1}$ (mean ± SE, $n = 3$), the $pH_{0.5}$ is 6.430 ± 0.009 (mean ± SE, $n = 3$), and the $n$ coefficient is 6 (Fig. 1 *B*). These data reflect that the transition from the closed state to the open state for the BvPIP2;2 homotetramer shows the same cooperative response as the heterotetramer, but it occurs at a higher proton concentration ($p < 0.0001$).

We have also compared the activity profile of oocytes injected with 5 ng of heterodimer cRNA with that obtained for oocytes coinjected with 2.5 ng of BvPIP2;2 cRNA plus 2.5 ng of BvPIP1;1 cRNA (Fig. 1 *B*). Results show that the maximal $P_f$, $pH_{0.5}$, and $n$ coefficient obtained for oocytes expressing the heterodimer are not different from the parameter values corresponding to the coexpression of BvPIP2;2 and BvPIP1;1 monomers (maximal $P_f$ of $(206.65 \pm 31.82) \times 10^{-4}$ cm $s^{-1}$, $pH_{0.5}$ of 6.787 ± 0.004, and $n$ coefficient of 5) (mean ± SE, $n = 5$) ($p > 0.05$). Despite this high similarity in responses, the injection of heterodimer gives a single heterotetrameric species, but coexpression of BvPIP2;2 and BvPIP1;1 monomers might result in up to five types of tetrameric species (Fig. S1). Considering that 1) homotetrameric BvPIP1;1 is not located in the plasma membrane (13,17), 2) BvPIP2;2 homotetramers present a low $P_f$ and $pH_{0.5}$ shifts toward acidic values (17), and 3) the dependence of $P_f$ on pH for the heterodimer and the coexpression are alike (Fig. 1 *B*), our results for (BvPIP1 + BvPIP2)-coinjected oocytes are compatible with different possibilities, for example, 1) the expression of heterotetramers with 2:2 stoichiometry only; 2) the expression of heterotetramers with 2:2, 1:3, and 3:1 stoichiometries and indistinguishable functional properties; or 3) the expression of heterotetramers with

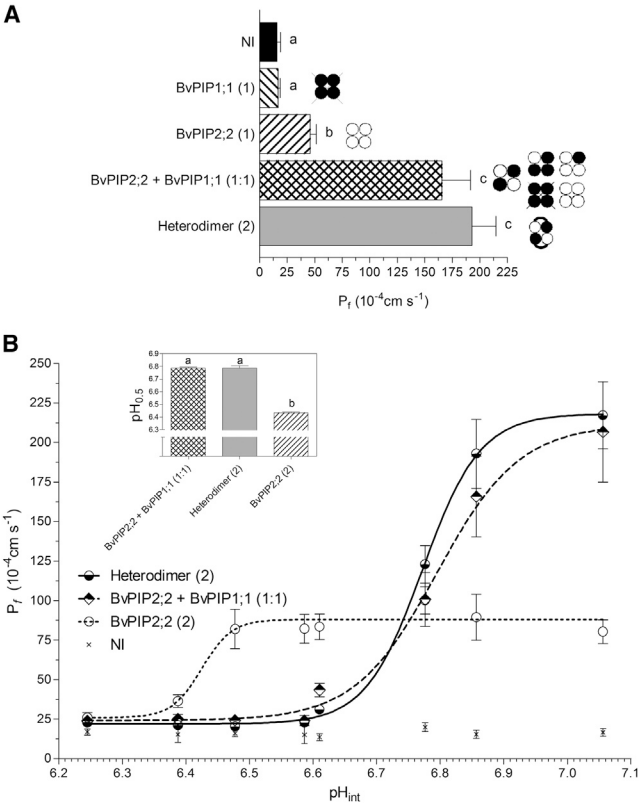


FIGURE 1 Dependence of osmotic water permeability ($P_f$) on oocyte internal pH for the coexpression of BvPIP1;1 and BvPIP2;2, single expressed heterodimer, and BvPIP2;2 monomer. (*A*) $P_f$ measurements of oocytes injected with different amounts of cRNA coding for BvPIP1;1, BvPIP2;2, and heterodimer, and coinjected BvPIP2;2 + BvPIP1;1 monomers. The amount of cRNA is shown in parentheses, where (1) is equivalent to 2.5ng, (2) is equivalent to 5 ng of cRNA per oocyte, and a (1:1) mass ratio corresponds to 2.5 ng of BvPIP2;2 cRNA plus 2.5 ng of BvPIP1;1 cRNA. NI, noninjected oocytes used as negative controls. The expression of BvPIP2;2 homotetramers leads to an increase in the plasma membrane osmotic water permeability coefficient ($P_f$) compatible with an active water channel, whereas the expression of BvPIP1;1 homotetramers does not, as they do not localize in the plasma membrane (17). Expression of heterodimer and coexpression of BvPIP2;2 with BvPIP1;1 monomers lead to comparable increases in $P_f$. Moreover, both are significantly different from the expression of BvPIP2;2 alone. Data are expressed as mean ± SE water permeability values ($n = 5$); 14–20 oocytes were tested for each treatment in each independent experiment. Letters a, b, and c denote significantly different ($p < 0.05$) values from each other as determined by the two-tailed Student's *t*-test. To the right of each bar is indicated, in cartoon format, the plausible heterotetrameric assemblies formed by injection of each cRNA. Crossed-out tetramers are those that are not located in the plasma membrane. BvPIP1;1 monomers is represented by solid circles, BvPIP2;2 monomers by open circles and the heterodimer by an open circle and a solid circle connected with a curved line. (*B*) $P_f$ behavior after cytosolic acidification was tested in oocytes injected with heterodimer cRNA (*solid line with semisolid circles*), coexpressed BvPIP2;2 and BvPIP1;1 (*dashed line with semisolid diamonds*) in a 1:1 mass ratio, or BvPIP2;2 cRNA alone (*dashed line with open circles*). The expression of heterodimers accounts for a different $pH_{int}$ sensitivity in comparison with oocytes expressing BvPIP2;2 alone, but not in comparison with oocytes coexpressing BvPIP2;2 and BvPIP1;1 monomers. The data points are representative values obtained from the same batch of oocytes (mean $P_f$ ± SE). The inset shows $pH_{0.5}$ values reported as the average of five independent experiments (mean ± SE, $n = 5$); 12–16 oocytes were tested for each condition in each independent experiment. Letters a and b denote values significantly different from each other ($p < 0.0001$), as determined by two-tailed Student's *t*-test.

2:2 stoichiometry plus heterotetrameric configurations 1:3 and 3:1 in low quantities.

As previous studies have shown that heterooligomeric channels can be packaged either with fixed or variable stoichiometry, it is important to determine whether, in the case of coexpression of BvPIPs, only 2:2 heteroteramers are able to assemble or variable conformations can be formed. For example, the stoichiometry of animal heteromeric $K^+$ channels has been well studied, and heterotetramers composed of Kv2.1 and the modulatory Kv9.3 present a fixed 3:1 stoichiometry (34). In contrast, variable subunit stoichiometry has been described for plant $K^+$ channels, where both 2:2 and 3:1 stoichiometries of KAT1:KDC1 heterotetramers are functional (28). Moreover, a work concerning the stoichiometry of acid-sensing ion channels in mammals (ASICs, a class of proton-gated cation channels) has shown that ASIC1a and ASIC2a randomly assemble into complexes with flexible stoichiometry that coexist with both homomers within the same cell (35,36).

In the case of PIP, two reports assume random heterotetramerization for both strawberry and tobacco PIP (6,7). If the coexpression of BvPIP2;2 and BvPIP1;1 gives random tetramers—as in the case of plant $K^+$ channels—different molecular species are expected to be formed. These possibilities will be further developed in the following sections.

## Heterotetramers with 3:1 and 1:3 stoichiometries are active channels able to localize at the plasma membrane

To investigate whether heterotetramer stoichiometries other than 2:2 can also be assembled, we coexpressed the heterodimer with BvPIP2;2 or BvPIP1;1 monomer. Moreover, with this experimental approach we could characterize the biological activity and localization of those species.

When the heterodimer is coexpressed with BvPIP2;2, three stoichiometries of tetramers are possible: 4:0 (the homotetrameric BvPIP2;2), 3:1 (three molecules of BvPIP2;2 and one of BvPIP1;1), and 2:2 (two molecules of BvPIP2;2 and two molecules of BvPIP1;1). On the other hand, when the heterodimer is coexpressed with BvPIP1;1, the possible assemblies at the plasma membrane are only the heterotetramers with 2:2 stoichiometry (two molecules of BvPIP2;2 and two of BvPIP1;1) and 1:3 stoichiometry (one molecule of BvPIP2;2 and three molecules of BvPIP1;1), since homotetramers of BvPIP1;1 are not able to reach the plasma membrane (13). Results show that the $P_f$ values for oocytes coinjected either with the heterodimer plus monomeric BvPIP2;2 cRNA or with the heterodimer plus monomeric BvPIP1;1 cRNA are both significantly different from the $P_f$ for oocytes injected only with the cRNA coding for the heterodimer alone

($p < 0.05$) (Fig. 2). This difference suggests the presence of heterotetramers with configurations different from 2:2 stoichiometry. The $P_f$ observed for the coinjection of the heterodimer plus monomeric BvPIP1;1, where homotetrameric BvPIP1;1 does not render water transport due to its internal cellular localization, provides strong evidence in favor of the 1:3 stoichiometry. In the case of the coinjection of heterodimer plus monomeric BvPIP2;2, the BvPIP2;2 homotetramer can also contribute to the whole-oocyte $P_f$, so the conclusion about the presence of the heterotetramers with 3:1 stoichiometry is not as straightforward as in the previous case. Nevertheless, considering that the $P_f$ of oocytes coexpressing the heterodimer plus monomeric BvPIP2;2 is higher than the $P_f$ rendered by the heterodimer alone—and at the same time different from the one obtained for oocytes coinjected with the heterodimer plus monomeric BvPIP1;1 ($p < 0.05$) (Fig. 2), we can presume the existence of heterotetramers with 3:1 and 2:2 stoichiometries together with BvPIP2;2 homotetramers at the oocyte plasma membrane.

Based on our previous results, we hypothesized that the differences between the biological responses of oocytes coexpressing the heterodimer with monomeric PIP2 and those coexpressing the heterodimer with PIP1 were due to the localization of PIP2/PIP1 homotetramers either in or out of the plasma membrane, respectively. This fact may contribute to increasing or decreasing, respectively, the whole-membrane water transport. To test this hypothesis, we assayed the cellular localization of fluorescently tagged BvPIP2;2 or BvPIP1;1 when coexpressed with heterodimers by confocal fluorescence microscopy (Fig. 3). First, we confirmed that the coexpression of the heterodimer with fluorescent monomers reproduced the functional pattern of wild-type AQPs (Fig. S3). As previously reported (13), BvPIP1;1-ECFP presents internal localization (in the same area of the TMR-dextran, a marker of the interior of the cell) (Fig. 3, *AIII* and *CIII*). On the other hand, fluorescence due to BvPIP2;2-EYFP is found on the edge of the cell, mostly in the plasma membrane (Fig. 3, *BIII* and *DIII*). In all cases where BvPIP1;1-ECFP or BvPIP2;2-EYFP are coexpressed with heterodimers, the fluorescence signal is detected mostly in the plasma membrane (Fig. 3, *AI, AII*, *BI*, and *BII*). Moreover, when BvPIP1;1-ECFP is present, the fluorescence signal is also observed in the interior of the cell (Fig. 3, *AI* and *AII*). This fluorescent pattern is compatible with 1) the presence of heterotetramers with 3:1 stoichiometry and homotetramers of BvPIP2;2 at the plasma membrane, for the case of oocytes coexpressing BvPIP2;2-EYFP with heterodimers (Fig. 3, *BI* and *BII*); and 2) the presence of heterotetrameric species with 1:3 stoichiometry at the plasma membrane and the BvPIP1;1 homotetramers in the interior of the cell, in the case of oocytes coexpressing heterodimer + BvPIP1;1-ECFP (Fig. 3, *AI* and *AII*).

In summary, functional assays together with localization data allow us to rule out a fixed heterotetramer stoichiometry for BvPIPs. Overall, the data show that BvPIP heterotetramers with 2:2, 3:1, and 1:3 stoichiometry are active channels that can be localized in the plasma membrane.

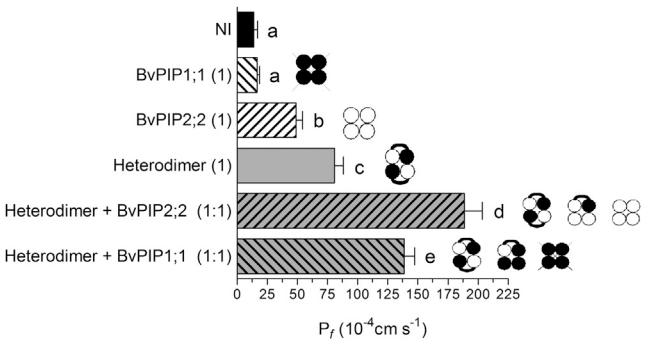


FIGURE 2 Osmotic water permeability of oocytes coexpressing BvPIP1;1 or BvPIP2;2 monomers with the heterodimer in a 1:1 mass ratio. $P_f$ measurements of oocytes injected with cRNA coding for BvPIP1;1, BvPIP2;2, heterodimer, heterodimer + monomer BvPIP1;1, and heterodimer + monomer BvPIP2;2. The amount of cRNA is shown in parentheses; where (1) is equivalent to 2.5 ng of cRNA per oocyte and a (1:1) mass ratio corresponds to 2.5 ng of one cRNA plus 2.5 ng of the other cRNA. NI, noninjected oocytes used as negative controls. Oocytes expressing the heterodimer show $P_f$ values significantly different from those of BvPIP2;2 cRNA alone. Coexpression of the heterodimer with BvPIP2;2 or BvPIP1;1 monomers in a 1:1 cRNA mass ratio show different properties in terms of membrane water permeability, stating that heterotetramers with diverse composition must be present in the plasma membrane. Data are mean (± SE) water permeability values ($n = 4$), and 14–18 oocytes were tested for each treatment in each independent experiment. Letters a–e denote values significantly different from each other ($p < 0.05$), as determined by the two-tailed Student's *t*-test. To the right of each bar is indicated, in cartoon format, the plausible heterotetrameric assemblies formed by injection of each cRNA. Crossed-out tetramers are those that are not located in the plasma membrane. BvPIP1;1 monomer is represented by a solid circle, BvPIP2;2 monomer by an open circle, and the heterodimer by an open circle and a solid circle connected with a curved line.

## Cooperativity in the proton-sensing response of different stoichiometric species

To gain insight into the biological relevance of the different heterotetrameric assemblies that may exist at the plasma membrane, we have found it useful to examine the proton sensing of heterotetramers comprising different stoichiometric ratios. We performed several coexpressions of the heterodimer with BvPIP2;2 or BvPIP1;1 monomers at different cRNA ratios to favor the assembly of 3:1 or 1:3 heteroteramer stoichiometry and studied the pH dependence of $P_f$ for the formed tetramers (Fig. 4).

Fig. 4, *A–C*, shows the cooperativity response and $pH_{0.5}$ of heterodimer coexpressed with BvPIP1;1 in three cRNA mass ratios: with equal parts of both cRNAs (2.5 ng of heterodimer plus 2.5 ng of BvPIP1;1; cRNA mass ratio, 1:1); with one part heterodimer plus two parts monomer (2.5 ng of heterodimer plus 5 ng of BvPIP1;1; cRNA mass ratio, 1:2); and with one part heterodimer plus four parts monomer (1.25 ng of heterodimer plus 5 ng of BvPIP1;1; cRNA mass ratio, 0.5:2).

For cRNA mass ratio 1:2, the maximal $P_f$ is lower than that observed for cRNA mass ratio 1:1 (Fig. 4 *A*), and the

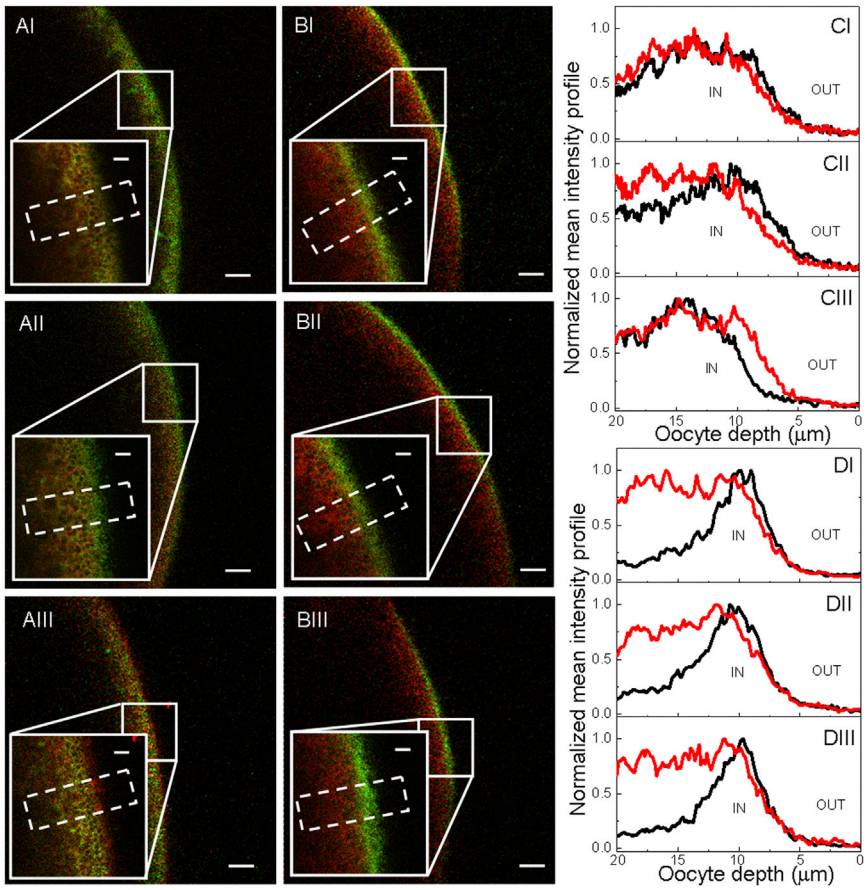


FIGURE 3 Cellular localization of BvPIP1;1-ECFP and BvPIP2;2-EYFP when coexpressed with heterodimer in *Xenopus laevis* oocytes. (*A*) Confocal images of an oocyte coexpressing the heterodimer with BvPIP1;1-ECFP in mass ratios of 1:2 (*AI*, *green*) and 1:1 (*AII*, *green*), or expressing BvPIP1;1-ECFP alone (*AIII*, *green*); oocytes were previously injected with TMR-dextran (*red*). (*B*) Confocal images of an oocyte coexpressing heterodimer with BvPIP2;2-EYFP in mass ratios of 1:2 (*BI*, *green*) and 1:1 (*BII*, *green*), or expressing BvPIP2;2-EYFP alone (*BIII*, *green*); oocytes were previously injected with TMR-dextran (*red*). The oocyte surface is near the right of each image frame, and the interior of the oocyte is to the left. (*Insets*) Enlargement of the indicated square section. Scale bar, 20 $\mu$m; inset scale bar, 5 $\mu$m. (*C* and *D*) Normalized mean intensity profiles of areas selected from each confocal image (*dashed white rectangles*). Graphs (*CI*)–(*CIII*) correspond to the mean intensity profiles of (*AI*)–(*AIII*), and graphs (*DI*)–(*DIII*) correspond to the mean intensity profiles of (*BI*)–(*BIII*), respectively. The black line corresponds to the ECFP or EYFP signal, and the red line to the TMR-dextran signal. IN/OUT indicates the interior/exterior of the cell, respectively. To see this figure in color, go online.

$pH_{0.5}$ value is not different (Fig. 4 *C*). When the amount of heterodimer is four times lower than that of monomeric BvPIP1;1 (cRNA mass ratio 0.5:2) (Fig. 4 *B*), the maximal $P_f$ is lower than that observed for cRNA mass ratios of 1:2, but the $pH_{0.5}$ is not different (Fig. 4 *C*). In addition, in all the coexpression ratios tested, the $n$ coefficient is equal to 6. The response found is compatible with the formation of increasing quantities of homotetrameric BvPIP1;1 when the cRNA of the BvPIP1;1 monomer is increased. As BvPIP1;1 homotetramer is not located in the plasma membrane, the maximal $P_f$ decreases, but even for a cRNA mass ratio of 0.5:2, the $P_f$ is different from the maximal $P_f$ observed for the heterodimer alone (Fig. 4 *B*). These results, taken together, are compatible with the presence of heterotetramers with 2:2 and 1:3 stoichiometry, all having the same cooperative response for proton sensing (Fig. 4 *C*).

Fig. 4, *D–F*, shows the cooperativity response and $pH_{0.5}$ of coexpressed heterodimer + BvPIP2;2 in three cRNA mass ratios, with equal parts of both cRNA (2.5 ng of heterodimer plus 2.5 ng of BvPIP2;2; cRNA mass ratio, 1:1); with one part heterodimer plus two parts monomer (2.5 ng of heterodimer plus 5 ng of BvPIP2;2; cRNA mass ratio, 1:2); and with one part heterodimer plus four parts monomer (1.25 ng of heterodimer plus 5 ng of BvPIP2;2; cRNA mass ratio, 0.5:2).

When the BvPIP2;2 cRNA mass injected is higher than the heterodimer cRNA mass (1:2 cRNA mass ratio), the maximal $P_f$ is lower than the maximal $P_f$ observed for a 1:1 cRNA mass ratio (Fig. 4 *D*), but $pH_{0.5}$ is not different (Fig. 4 *F*). In this case, the $n$ coefficient for the 1:2 cRNA mass ratio is ~3. These results suggest that the cooperativity is apparently lower when a higher quantity of monomeric BvPIP2;2 is added. Fig. 4 *E* shows the results obtained for coexpression of the heterodimer plus four times its quantity of monomeric BvPIP2;2 (cRNA mass ratio, 0.5:2). In this case, maximal $P_f$ is lower than that observed for 1:2 cRNA mass ratios (Fig. 4 *E*) and $pH_{0.5}$ shifts toward acidic values (Fig. 4 *F*). These results are compatible with a stronger presence of BvPIP2;2 homotetramer when the mass of BvPIP2;2 cRNA is higher than the mass of heterodimer cRNA. This fact is well distinguished for this extreme cRNA mass ratio (0.5:2), since the curve for water transport pH dependence resembles the curve corresponding to the expression of BvPIP2;2 homotetramers alone (Fig. 4 *E*).

In addition, it must be stressed that the $pH_{0.5}$ values and $n$ coefficients for heterodimers expressed alone ($pH_{0.5}$ = 6.785 ± 0.009; $n$ = 6) and heterodimers coexpressed with monomeric BvPIP1;1 or BvPIP2;2 in a 1:1 cRNA mass ratio (Fig. 4, *A* and *D*, respectively) are not different.

The overall results presented not only support that PIP heterotetrameric channels have no preferred composition,

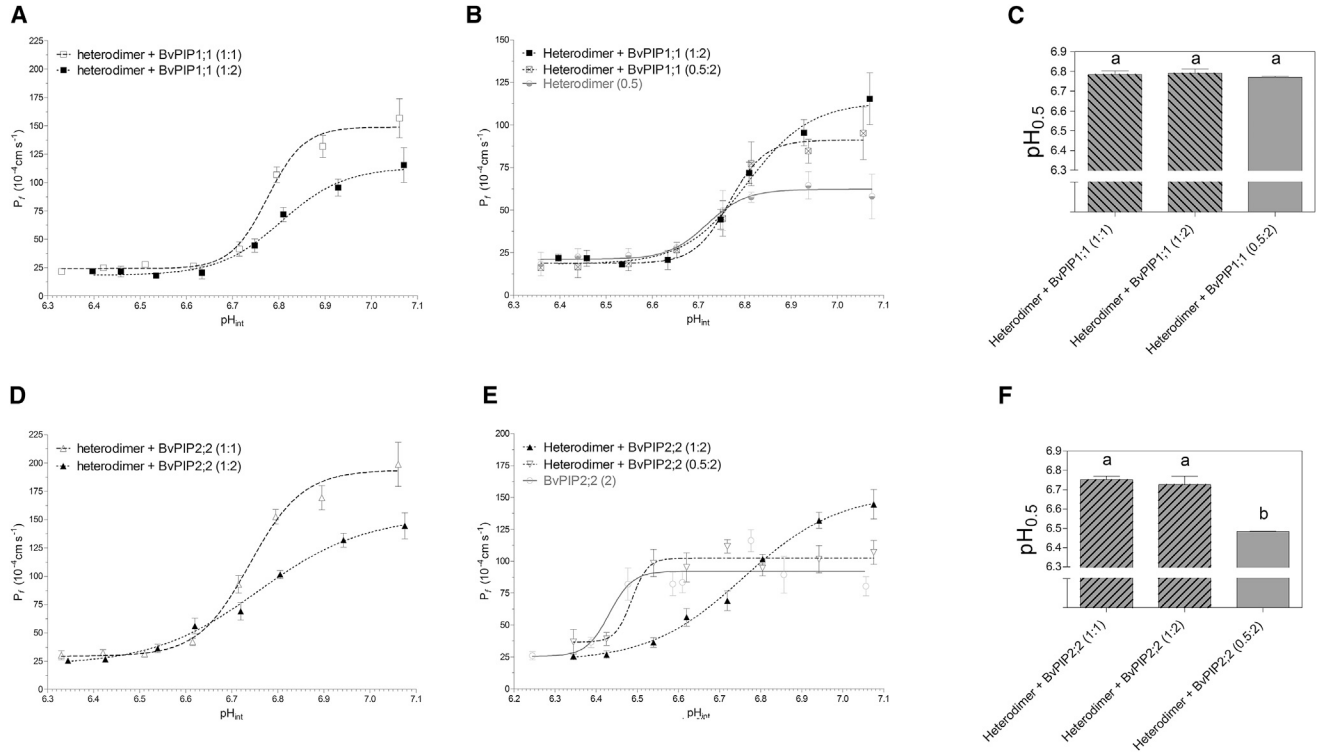


FIGURE 4 $P_f$ dependence on pH for heterodimer plus BvPIP1;1 or BvPIP2;2 monomers at different cRNA mass ratios. (*A* and *B*) pH dose-response curves of the plasma membrane $P_f$ of oocytes coexpressing BvPIP1;1 monomers with the heterodimer in different cRNA mass ratios (1:1, 1:2, and 0.5:2). $P_f$ behavior after cytosolic acidification was tested in oocytes coinjected with BvPIP1;1 monomers in 1:1 (*dashed line*, *open squares*) (*A*), 1:2 (*dashed line*, *solid squares*) (*A* and *B*), and 0.5:2 cRNA mass ratios (*dashed line*, *crossed-out squares*) (*B*). For comparison, we also show the pH dose-response curve of oocytes expressing heterodimer cRNA alone in low cRNA mass quantity (*B*) (*solid line*, *semisolid circles*). For each condition, mean values are shown as the mean $P_f \pm$ SE for $n = 8$–12 oocytes tested in each independent experiment. (*C*) Mean $pH_{0.5} \pm$ SE of the fitting curves for $n = 3$–5 independent experiments; $pH_{0.5}$ values are not significantly different from each other, as determined by the two-tailed Student's *t*-test ($p > 0.05$). (*D* and *E*) pH dose-response curves of the plasma membrane $P_f$ of oocytes coexpressing BvPIP2;2 monomers with the heterodimer in different mass ratios (1:1, 1:2, and 0.5:2). $P_f$ behavior after cytosolic acidification was tested in oocytes injected with heterodimer cRNA alone or coinjected with BvPIP2;2 monomers in 1:1 (*dashed line*, *open triangles*) (*D*), 1:2 (*dashed line*, *solid triangles*) (*D* and *E*), or 0.5:2 cRNA mass ratios (*dashed line*, *open inverted triangles*) (*E*). For comparison, the pH dose-response curve of oocytes expressing BvPIP2;2 alone is also shown (*solid line, open circles*) (*E*). For each condition, mean values are shown as the mean $P_f \pm$ SE for $n = 8$–12 oocytes tested in each independent experiment. (*F*) Mean $pH_{0.5} \pm$ SE of the fitting curves for $n = 3$–5 independent experiments; letters a and b indicate values significantly different from each other, as determined by the two-tailed Student's *t*-test ($p > 0.05$).

but also experimentally prove that the abundance of the different heterotetrameric species depends on the relative expression of PIP monomers. According to our results, other reports have shown that the heterooligomerization of proteins is random and depends on the relative subunit expression level, i.e., variable stoichiometries have been reported with no constraint in the subunit arrangement (35,37–39). Interestingly, despite the presence of different monomers, all heterotetrameric configurations (3:1, 2:2, and 1:3) present equivalent biological activity in terms of pH gating and cooperativity response for water transport.

## PIP heterotetramers having 2:2, 1:3, and 3:1 stoichiometries contribute equally to the total plasma-membrane $P_f$

To predict the contribution of each tetrameric form to the whole plasma membrane permeability, we have developed a mathematical model of PIP1-PIP2 assembly. To construct the model, we took into account that tetramerization occurs by random dimerization of dimers, and thus, a binomial distribution was applied.

As the expression of PIP1, PIP2, or PIP2-PIP1 heterodimer forms only one type of tetramer, we can experimentally obtain the $P_f$ contribution of these tetramers. For a 2:2 heterotetramer, the $P_f$ contribution is $(34.46 \pm 4.31) \times 10^{-4}$ cm $s^{-1}$ $ng^{-1}$ (mean $\pm$ SE, $n = 6$); for a PIP2 homotetramer, the corresponding value is $(14.86 \pm 2.07) \times 10^{-4}$ cm $s^{-1}$ $ng^{-1}$ (mean $\pm$ SE, $n = 5$); and for a PIP1 homotetramer, the $P_f$ contribution is null. Then, we can estimate the $P_f$ contribution of 1:3 and 3:1 tetrameric species, considering the experimental results of the coexpression experiments with different cRNA ratios of PIP2-PIP1 heterodimer plus PIP2 or PIP1 (Figs. 2 and 4). For this, we estimated first the predicted fraction of each tetrameric species produced by different ratios

of PIP1 or PIP2 cRNA injected (Fig.S4). Then, by fitting the model to our experimental data, we determined the individual $\Omega_i$ of heterotetramers with 1:3 or 3:1 stoichiometry as $(28.45 \pm 2.74) \times 10^{-4}$ cm $s^{-1}$ $ng^{-1}$ (mean $\pm$ SD, $n = 3$) and $(30.25 \pm 3.70) \times 10^{-4}$ cm $s^{-1}$ $ng^{-1}$ (mean $\pm$ SD, $n = 3$), respectively (Fig. 5, *A* and *B*, respectively). In conclusion, the $P_f$ contribution of heterotetramers having 2:2, 1:3, or 3:1 stoichiometry to the total plasma membrane $P_f$ is not significantly different ($p < 0.05$). Moreover, the single contribution of each tetrameric species to the total osmotic plasma membrane permeability ($P_f$) has been estimated taking into account the probability of formation of each single tetrameric species (Fig. S4) and the $P_f$ contribution of each specie ($\Omega_i$) as a function of the molar fraction of PIP1 (Fig. 5 *C*) or PIP2 (Fig. 5 *D*).

Our results indicate that all PIP2-PIP1 heterotetrameric species have the same water permeability behavior, presenting major differences from the homotetramers. Interestingly, the contribution of PIP heterotetramers is twice the contribution of PIP2 homotetramers. Of course, we cannot rule out that the different heterotetrameric configurations studied here present differences in solute selectivity, as has been shown to occur for tobacco PIP (7).

## CONCLUSIONS

By means of complementary experimental approaches (swelling assays, cellular localization by confocal fluorescence microscopy, cooperativity on water transport modulation by pH, and mathematical modeling analysis), we have proved that configurations 3:1, 1:3, and 2:2 of BvPIP2;2 and BvPIP1;1 heterotetramers coexist and are all able to reach the plasma membrane. All these heterotetrameric species have equivalent biological activity in terms of water transport, pH regulation, and cooperative response. Furthermore, the contribution of any heterotetrameric assembly to the total water transport through the plasma membrane doubles the contribution of PIP2 homotetramers. Also, the pH gating of all heterotetramers is given at lower proton concentrations in comparison with PIP2 homotetramers.

Our results also show how the cell plasma membrane water permeability can be modulated from low $P_f$ values to high $P_f$ values depending on the relative expression of PIP1 and PIP2. If one PIP monomer (PIP1 or PIP2) outnumbers the other, the assembly of 1:3 (or 3:1) heterotetramers or even PIP1/PIP2 homotetramers is favored. Thus, our findings prove that the assembly of PIP1 and PIP2 tetramers is flexible and dependent on the availability of PIP1 and PIP2 molecules, allowing the cell to tightly control the water transport through the plasma membrane.

## SUPPORTING MATERIAL

Four figures are available at http://www.biophysj.org/biophysj/supplemental/S0006-3495(16)00135-1.

## AUTHOR CONTRIBUTIONS

C.J., N.A., L.G.F., and K.A. designed the research. C.J., L.S., F.S., G.S., N.A., and F.L.G.F. performed the experiments. C.J., L.S., F.S., G.S., N.A., L.P., G.A., F.L.G.F., and K.A. analyzed the data. N.A., G.S., and F.L.G.F. contributed analytical and computational tools. C.J., G.S., N.A., F.L.G.F., and K.A. wrote the manuscript.

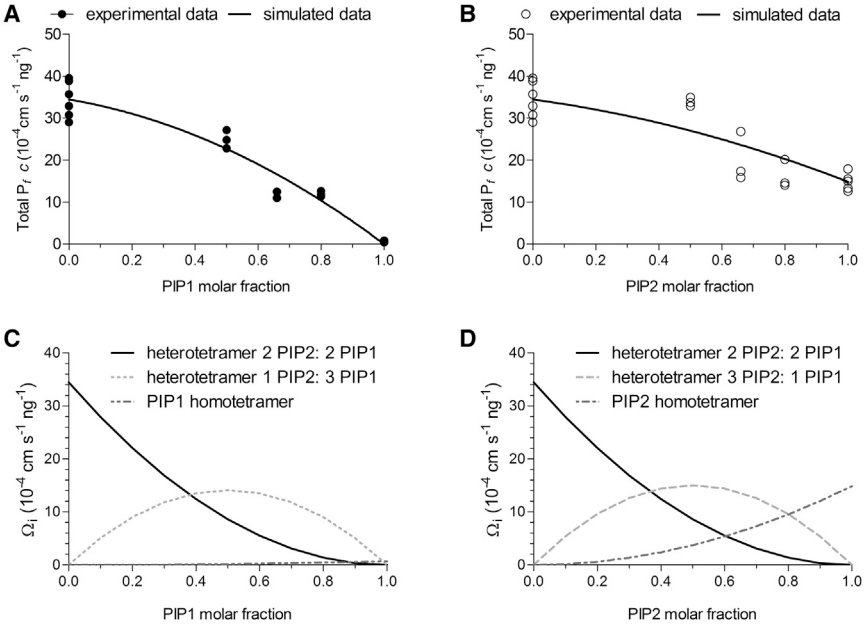


FIGURE 5 (*A* and *B*) Total $P_f$ *c* measured (experimental data) or estimated (simulated data) as a function of the molar fraction of PIP1 (*A*) or PIP2 (*B*). Equation 3 was fitted to the data from experiments done by coexpression of heterodimers plus PIP1 (X + Y), and Eq. 4 was fitted to data from experiments done by coexpression of heterodimers plus PIP2 (X + Z); $R^2 = 0.9360$ and 0.7586, respectively. (*C* and *D*) $P_f$ of each tetrameric species formed at the plasma membrane ($\Omega$) as a function of the molar fraction of PIP1 (*C*) or PIP2 (*D*). $\Omega_i$ = ($P_f$ given by a single tetrameric species – $P_f$ of noninjected oocytes)/injected ng of total cRNA; $\Omega_{2:2}$, $\Omega_{0:4}$, and $\Omega_{4:0}$ $P_f$ values were obtained experimentally, whereas $\Omega_{1:3}$ and $\Omega_{3:1}$ are parameters obtained by fitting Eq. 3 or Eq. 4, respectively, to the experimental data by nonlinear regression using GraphPad Prism 5.02 software.

## ACKNOWLEDGMENTS

We thank Nicolas San Martin for design assistance.

This work was supported by the Agencia Nacional de Promoción Científica y Tecnológica (Grant PICT 2010 02042 to K.A., PICT 2011 2239 to G.A., PICT 2010 0457 to L.P., and PICT 2013 1691 to F.L.G.F.) and Universidad de Buenos Aires (UBACYT Grant 0159-2013 to K.A., 0784-2014 to G.A., 0155 to L.P., and 0460-2014 to F.L.G.F.).

## REFERENCES

1. Shi, L. B., W. R. Skach, and A. S. Verkman. 1994. Functional independence of monomeric CHIP28 water channels revealed by expression of wild-type mutant heterodimers. *J. Biol. Chem.* 269:10417–10422.
2. Abascal, F., I. Irisarri, and R. Zardoya. 2014. Diversity and evolution of membrane intrinsic proteins. *Biochim. Biophys. Acta.* 1840:1468–1481.
3. Kukulski, W., A. D. Schenk, …, A. Engel. 2005. The 5A structure of heterologously expressed plant aquaporin SoPIP2;1. *J. Mol. Biol.* 350:611–616.
4. Fotiadis, D., P. Jenö, …, A. Engel. 2001. Structural characterization of two aquaporins isolated from native spinach leaf plasma membranes. *J. Biol. Chem.* 276:1707–1714.
5. Fetter, K., V. Van Wilder, …, F. Chaumont. 2004. Interactions between plasma membrane aquaporins modulate their water channel activity. *Plant Cell.* 16:215–228.
6. Yaneff, A., L. Sigaut, …, G. Amodeo. 2014. Heteromerization of PIP aquaporins affects their intrinsic permeability. *Proc. Natl. Acad. Sci. USA.* 111:231–236.
7. Otto, B., N. Uehlein, …, R. Kaldenhoff. 2010. Aquaporin tetramer composition modifies the function of tobacco aquaporins. *J. Biol. Chem.* 285:31253–31260.
8. Hachez, C., A. Besserer, …, F. Chaumont. 2013. Insights into plant plasma membrane aquaporin trafficking. *Trends Plant Sci.* 18:344–352.
9. Zelazny, E., U. Miecielica, …, F. Chaumont. 2009. An N-terminal diacidic motif is required for the trafficking of maize aquaporins ZmPIP2;4 and ZmPIP2;5 to the plasma membrane. *Plant J.* 57:346–355.
10. Sorieul, M., V. Santoni, …, D. T. T. Luu. 2011. Mechanisms and effects of retention of over-expressed aquaporin AtPIP2;1 in the endoplasmic reticulum. *Traffic.* 12:473–482.
11. Chevalier, A. S., G. P. Bienert, and F. Chaumont. 2014. A new LxxxA motif in the transmembrane Helix3 of maize aquaporins belonging to the plasma membrane intrinsic protein PIP2 group is required for their trafficking to the plasma membrane. *Plant Physiol.* 166:125–138.
12. Zelazny, E., J. W. Borst, …, F. Chaumont. 2007. FRET imaging in living maize cells reveals that plasma membrane aquaporins interact to regulate their subcellular localization. *Proc. Natl. Acad. Sci. USA.* 104:12359–12364.
13. Jozefkowicz, C., P. Rosi, …, K. Alleva. 2013. Loop A is critical for the functional interaction of two *Beta vulgaris* PIP aquaporins. *PLoS One.* 8:e57993.
14. Hachez, C., R. B. Heinen, …, F. Chaumont. 2008. The expression pattern of plasma membrane aquaporins in maize leaf highlights their role in hydraulic regulation. *Plant Mol. Biol.* 68:337–353.
15. Hachez, C., M. Moshelion, …, F. Chaumont. 2006. Localization and quantification of plasma membrane aquaporin expression in maize primary root: a clue to understanding their role as cellular plumbers. *Plant Mol. Biol.* 62:305–323.
16. Vandeleur, R. K., G. Mayo, …, S. D. Tyerman. 2009. The role of plasma membrane intrinsic protein aquaporins in water transport through roots: diurnal and drought stress responses reveal different strategies between isohydric and anisohydric cultivars of grapevine. *Plant Physiol.* 149:445–460.
17. Bellati, J., K. Alleva, …, G. Amodeo. 2010. Intracellular pH sensing is altered by plasma membrane PIP aquaporin co-expression. *Plant Mol. Biol.* 74:105–118.
18. Dreyer, I., S. Antunes, …, R. Hedrich. 1997. Plant $K^+$ channel $\alpha$-subunits assemble indiscriminately. *Biophys. J.* 72:2143–2150.
19. Geiger, D., D. Becker, …, R. Hedrich. 2009. Heteromeric AtKC1·AKT1 channels in Arabidopsis roots facilitate growth under $K^+$-limiting conditions. *J. Biol. Chem.* 284:21288–21295.
20. Jeanguenin, L., C. Alcon, …, A. A. Véry. 2011. AtKC1 is a general modulator of Arabidopsis inward *Shaker* channel activity. *Plant J.* 67:570–582.
21. Duby, G., E. Hosy, …, J. B. Thibaud. 2008. AtKC1, a conditionally targeted *Shaker*-type subunit, regulates the activity of plant $K^+$ channels. *Plant J.* 53:115–123.
22. Reintanz, B., A. Szyroki, …, R. Hedrich. 2002. AtKC1, a silent Arabidopsis potassium channel $\alpha$-subunit modulates root hair $K^+$ influx. *Proc. Natl. Acad. Sci. USA.* 99:4079–4084.
23. Zhang, R. B., and A. S. Verkman. 1991. Water and urea permeability properties of *Xenopus* oocytes: expression of mRNA from toad urinary bladder. *Am. J. Physiol.* 260:C26–C34.
24. Agre, P., J. C. Mathai, …, G. M. Preston. 1999. Functional analyses of aquaporin water channel proteins. *Methods Enzymol.* 294:550–572.
25. Brooks, J. M., and G. M. Wessel. 2003. Selective transport and packaging of the major yolk protein in the sea urchin. *Dev. Biol.* 261:353–370.
26. Kemmer, G., and S. Keller. 2010. Nonlinear least-squares data fitting in Excel spreadsheets. *Nat. Protoc.* 5:267–281.
27. Cattoni, D. I., O. Chara, …, F. L. González Flecha. 2015. Cooperativity in binding processes: new insights from phenomenological modeling. *PLoS One.* 10:e0146043. http://dx.doi.org/10.1371/journal.pone.0146043.
28. Naso, A., R. Montisci, …, C. Picco. 2006. Stoichiometry studies reveal functional properties of KDC1 in plant shaker potassium channels. *Biophys. J.* 91:3673–3683.
29. Veerappan, A., F. Cymer, …, D. Schneider. 2011. The tetrameric $\alpha$-helical membrane protein GlpF unfolds via a dimeric folding intermediate. *Biochemistry.* 50:10223–10230.
30. Naranjo, D. 1997. Assembly of Shaker K-Channels from a random mixture of subunits carrying different mutations. *In* From Ion Channels to Cell-to-Cell Conversations. Plenum Press, New York, pp. 35–46.
31. Ding, S., L. Ingleby, …, R. Horn. 2005. Investigating the putative glycine hinge in *Shaker* potassium channel. *J. Gen. Physiol.* 126:213–226.
32. Németh-Cahalan, K. L., D. M. Clemens, and J. E. Hall. 2013. Regulation of AQP0 water permeability is enhanced by cooperativity. *J. Gen. Physiol.* 141:287–295.
33. Tournaire-Roux, C., M. Sutka, …, C. Maurel. 2003. Cytosolic pH regulates root water transport during anoxic stress through gating of aquaporins. *Nature.* 425:393–397.
34. Kerschensteiner, D., F. Soto, and M. Stocker. 2005. Fluorescence measurements reveal stoichiometry of $K^+$ channels formed by modulatory and delayed rectifier $\alpha$-subunits. *Proc. Natl. Acad. Sci. USA.* 102:6160–6165.
35. Bartoi, T., K. Augustinowski, …, M. H. Ulbrich. 2014. Acid-sensing ion channel (ASIC) 1a/2a heteromers have a flexible 2:1/1:2 stoichiometry. *Proc. Natl. Acad. Sci. USA.* 111:8281–8286.
36. Gründer, S., and M. Pusch. 2015. Biophysical properties of acid-sensing ion channels (ASICs). *Neuropharmacology.* 94:9–18.
37. Wang, W., J. Xia, and R. S. Kass. 1998. MinK-KvLQT1 fusion proteins, evidence for multiple stoichiometries of the assembled IsK channel. *J. Biol. Chem.* 273:34069–34074.
38. Barrera, N. P., R. M. Henderson, …, J. M. Edwardson. 2007. The stoichiometry of P2X2/6 receptor heteromers depends on relative subunit expression levels. *Biophys. J.* 93:505–512.
39. Stewart, A. P., J. C. Gómez-Posada, …, J. M. Edwardson. 2012. The Kv7.2/Kv7.3 heterotetramer assembles with a random subunit arrangement. *J. Biol. Chem.* 287:11870–11877.